
Unified Autoregressive Visual Generation and Understanding with Continuous Tokens

Lijie Fan^{1,*} Luming Tang^{1,*} Siyang Qin^{1,*} Tianhong Li² Xuan Yang¹ Siyuan Qiao¹
Andreas Steiner¹ Chen Sun¹ Yuanzhen Li¹ Tao Zhu¹ Michael Rubinstein¹ Michalis Raptis¹
Deqing Sun^{1,†} Radu Soricut^{1,†}

¹Google DeepMind ²MIT *[†] equal contribution

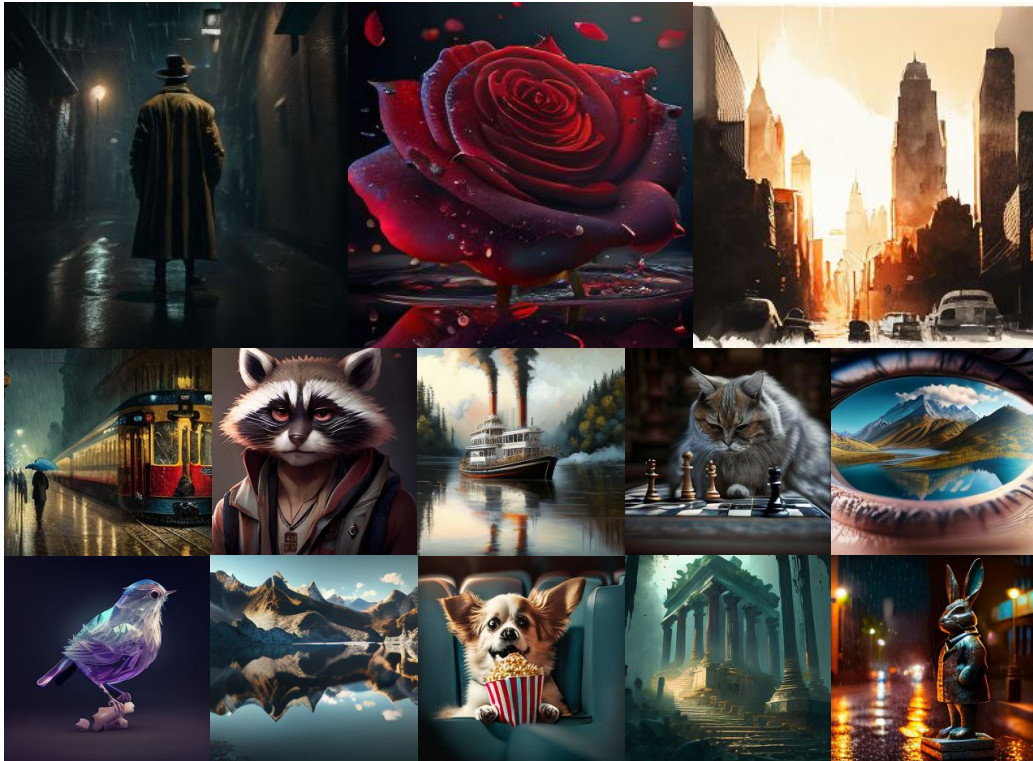


Figure 1: Generated images from our UniFluid autoregressive model after aesthetic finetuning.

Abstract

We present UniFluid, a unified autoregressive framework for joint visual generation and understanding leveraging continuous visual tokens. Our unified autoregressive architecture processes multimodal image and text inputs, generating discrete tokens for text and continuous tokens for image. We find though there is an inherent trade-off between the image generation and understanding task, a carefully tuned training recipe enables them to improve each other. By selecting an appropriate loss balance weight, the unified model achieves results comparable to or exceeding those of single-task baselines on both tasks. Furthermore, we demonstrate that employing stronger pre-trained LLMs and random-order generation during training is important to achieve high-fidelity image generation within this unified framework. Built upon the Gemma model series, UniFluid exhibits competitive performance across both image generation and understanding, demonstrating strong transferability to various downstream tasks, including image editing for generation, as well as visual captioning and question answering for understanding.

1 Introduction

Large Language Models (LLMs) have recently advanced from text-centric architectures, such as BERT [11] and GPT [35], toward multimodal systems capable of understanding and generating content across different modalities. GPT-3 [5] and PaLM [9] show that scaling language models leads to emergent capabilities, while Flamingo [2] further demonstrates that incorporating visual inputs facilitates unified multimodal reasoning. This trend toward unified vision-language model—using a single model for diverse tasks of visual understanding and generation—has promising potential for leveraging knowledge and reasoning abilities that transfer across different vision and language tasks, ultimately facilitating more robust and generalizable multimodal representation and modeling capabilities.

Motivated by the advantages and strong scaling properties of autoregressive models, coupled with their simplicity, we investigate a pure autoregressive framework for unified visual generation and understanding, without the limitations introduced by vector quantization (VQ). In this paper, we introduce UniFluid, a unified framework that leverages continuous visual tokens within an autoregressive architecture to jointly handle vision-language generation and understanding tasks. Building upon pre-trained Gemma [48] on large-scale text corpus, UniFluid unlocks powerful visual generation and understanding capabilities through training with paired image-text data, and further allows these two tasks to mutually benefit each other within a single architecture.

Specifically, UniFluid adopts a unified autoregressive framework where both text and continuous visual inputs are embedded as tokens in the same space, enabling seamless joint training of image generation and understanding tasks. UniFluid integrates a continuous tokenizer [12, 21] for image generation and a pre-trained SigLIP [59] image encoder for understanding tasks, while textual inputs are processed using a standard SentencePiece tokenizer [20]. The resulting multimodal sequences are modeled autoregressively using Gemma [48] as the underlying transformer backbone. Task-specific prediction heads—a diffusion-based head for image generation and a cross-entropy head for text generation—ensure effective modality-specific training and inference, enabling UniFluid to efficiently learn shared representations that mutually enhance its generation and understanding capabilities.

Our experiments demonstrate several key advantages of the proposed unified training strategy. We find though there is a trade-off between the two tasks, a carefully tuned training recipe can allow the tasks to support each other and outperform the single-task baselines. Effectively balancing the loss between the tasks allows a single model that performs both with results superior to or on par with single-task models. Moreover, the choice of pre-trained LLM backbone significantly impacts visual generation performance. We also find that while employing random generation order is essential for high-quality image synthesis, it is less critical for understanding tasks. Finally, our unified pre-trained models show strong generalization and transferability, achieving compelling results in downstream applications, including image editing and various vision-language understanding benchmarks.

2 Related Works

Multimodal Large Language Models. Multimodal Large Language Models [2, 10, 23, 26, 25, 3, 42] have shown significant performance in visual understanding tasks. Flamingo [2] adopted a frozen LLM and vision encoder, utilizing perceiver with cross-attention to bridge the modalities. LLaVA [26, 25] proposed instruction tuning over pre-trained LLMs with multimodal inputs to align a pre-trained image encoder into the LLM’s embedding space, thereby enabling it with visual understanding and instruction following capabilities. MiniGPT-4 [62] and mPLUG-Owl [56] have shown vision encoders can be connected to LLMs through projection layers, demonstrating sophisticated visual reasoning capabilities. The PaliGemma [3, 42] series built upon the Gemma [47, 48] model family to develop versatile vision-language models capable of strong transfer to diverse downstream visual understanding tasks.

Autoregressive Image Generation. While diffusion models [41, 36] have achieved impressive success in image generation, autoregressive image generation methods have also shown significant development, driven by their simplicity and closeness to LLM training paradigms. A large body of research centers on tokenizing images into discrete tokens and applying autoregressive objectives to these discrete representations. Notable examples include Parti [57] and Muse [6]. [49] proposes an approach that operates on image scales, progressively refining resolutions from coarse to fine through

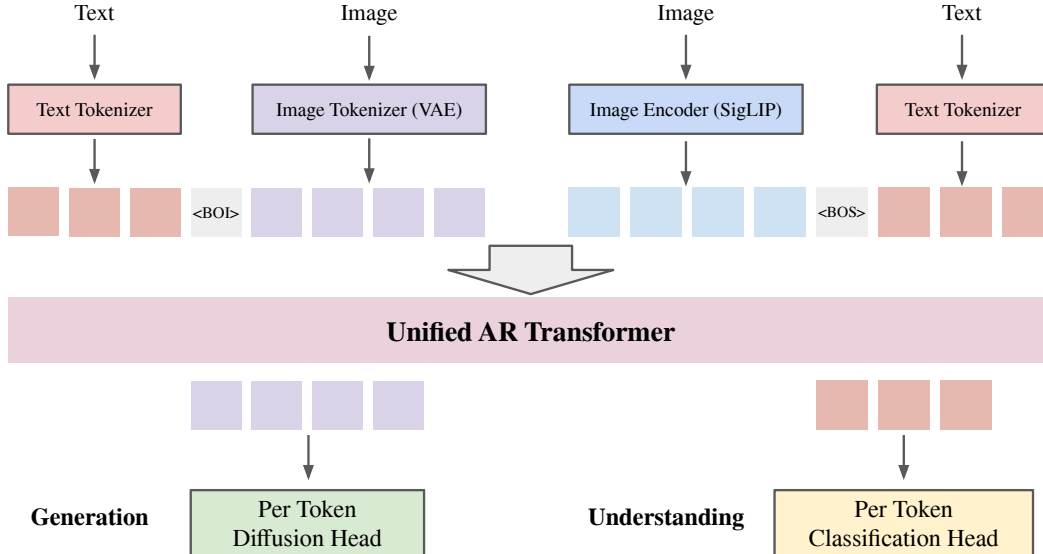


Figure 2: High-level illustration of UniFluid. UniFluid performs joint training of image generation and understanding tasks through next token prediction. For image embeddings, we use a VAE image tokenizer for generation, and a SigLIP image encoder for understanding. BOI/BOS stands for beginning of Image/Sentence.

next-scale prediction. Alternatively, works such as MAR [21], Fluid [12], and techniques employing per-token diffusion heads on top of LLM-predicted embeddings have explored autoregressive image generation with continuous visual tokens.

Unified Multimodal Models. There is growing research interests in unifying visual generation and understanding within a single model. VQ-based models, such as Chameleon [46], Emu [44], and Janus [54, 8], propose encoding visual inputs into discrete tokens and unifying tasks into next-token prediction within this discrete token space. Models with hybrid training targets, such as Transfusion [61, 38] and Show-O [55], aim to unify next-token prediction objectives with diffusion objectives within a single framework. MetaMorph [50] maintains the autoregressive objective by regressing visual SigLIP [59] features using an LLM, but necessitates a separate diffusion model to decode the predicted latent features into images. Our approach distinguishes itself by performing per-token autoregressive generation using continuous visual tokens. This maintains the next-token prediction objective, while not being limited by the vector quantized tokens. [45] also explores using continuous tokens to generate multimodal outputs.

3 Method

In this section, we illustrate the architecture of our UniFluid model. The model expects both image and text sequences as input and achieves joint training on both generation and understanding tasks, using next-token prediction as its training objective.

3.1 Unified Autoregressive Modeling with Continuous Visual Tokens

Our approach leverages the autoregressive paradigm to unify visual understanding and generation within a single framework. Given an ordered sequence of tokens $X = \{x^1, \dots, x^n\}$, the autoregressive model [34, 14, 51, 52] factorizes the joint probability distribution as a product of conditional probabilities, effectively framing the generation task as a sequential “next token prediction” problem: $p(X) = \prod_{i=1}^n p(x^i | x^1, \dots, x^{i-1})$. As shown in MAR [21] and Fluid [12], this autoregressive formulation is applicable for both discrete tokens and continuous tokens. In UniFluid, we exploit this property to enable the generation of continuous visual tokens under the unified decoder-only framework. Our model is modality-agnostic; both text and image tokens are treated as elements within a long unified sequence, and their respective logits are predicted iteratively in an autoregressive manner by the backbone transformer.

To accommodate the distinct nature of text and image modalities, we employ modality-specific prediction heads to calculate the appropriate loss functions and sampling for each modality. This unified approach allows the model to learn a shared representation space through the unified training procedure, facilitating synergistic learning and enabling seamless transitions between visual generation and understanding.

3.2 Architecture

As depicted in Figure 2, UniFluid employs a unified framework where both text and image inputs are tokenized and projected into a shared embedding space. This allows it to leverage a decoder-only transformer as the core backbone for the unified autoregressive task. Text inputs are tokenized using the SentencePiece tokenizer. This results in discrete tokens with a vocabulary size of V . For image generation, images are encoded into continuous visual tokens using a continuous variational autoencoder. To facilitate the process of image understanding, following PaliGemma, we used SigLIP as a separate image encoder to extract high-level information from the visual inputs. UniFluid consists of a classification head to convert the transformer’s text logits into a categorical distribution, and a diffusion head to convert image logits into a per-token probability distribution.

The inherent structure of text as a linear sequence aligns well with the standard 1D positional embeddings of the LLM, which are sufficient for text modeling and image understanding tasks. However, image tokens possess a 2D spatial structure. To capture this inherent 2D nature, we incorporate learnable 2D positional embeddings, which are added to the image token embeddings. Meanwhile, inspired by [58], to achieve random order generation, a position embedding for the next predicted token is also added to each image token. To enhance the model’s ability to initiate and guide image generation, we prepend a "Beginning of Image" (BOI) token to the sequence of continuous image tokens. This BOI token serves as a distinct signal, indicating the start of the visual generation process. Given that the sequence length for generated image tokens is predefined (256 tokens for 256x256 images), an explicit "End of Image" token is unnecessary in our case.

4 Implementation

4.1 Training

Per-token Classification Head for Discrete Text Tokens. We employ the same SentencePiece tokenizer as Gemma for text tokenization. The transformer’s output logits for text are transformed into categorical probability distributions over the vocabulary, and we apply the standard cross-entropy loss, denoted as L_{Text} , to optimize the prediction of these discrete text tokens.

Per-token Diffusion Head for Continuous Visual Tokens. We adopt the same continuous tokenizer as Fluid to embed 256x256 images into 32x32x4 continuous tokens, and use a patch size of 2 to merge 4 tokens into one. To model the per-token distribution of these predicted continuous visual tokens, we employ a lightweight MLP as a diffusion head. We adopt the same diffusion process and loss function, denoted as \mathcal{L}_{Visual} , as in [21, 12], which is specifically tailored for continuous visual token prediction. For the understanding task, the input image resolution is 224x224, and we use SigLIP as the image encoder. Note that the SigLIP features are only used as prefix for the understanding task during training, and no losses are added on top of them.

Task-Specific Training Configurations.

Image Understanding: For image understanding tasks, the model is provided with image embeddings and question tokens as input prefix. Following PaliGemma, we apply a bidirectional attention mask to both image and question tokens. A causal attention mask is applied to the answer tokens, ensuring that the model only attends to previous answer tokens during autoregressive generation. The text token loss, \mathcal{L}_{Text} , is calculated specifically on the answer text tokens.

Image Generation: Conversely, for image generation tasks, text prompts are provided as conditioning inputs. To maintain the appropriate information flow, we employ a bidirectional attention mask for the text prompt tokens, enabling them to attend to all other text tokens. A causal attention mask is applied to the image tokens, ensuring that each image token only attends to preceding image tokens. The visual token loss, \mathcal{L}_{Visual} , is calculated on the generated image tokens.

Unified Loss Function. The total training loss for UniFluid is a weighted sum of the text token prediction loss and the visual token prediction loss, defined as: $\mathcal{L} = \mathcal{L}_{Visual} + \lambda \cdot \mathcal{L}_{Text}$ where λ is a hyper-parameter that represents the weight assigned to the text token prediction loss, allowing us to balance the contributions of the two modalities during training.

Training Details. We train the model with a batch size of 2048 using the AdamW optimizer with a learning rate of $1e-4$. The training process consists of 1 million steps with a constant learning rate schedule and a warm-up period of 65k steps. Following [58], for image generation, the image token order is randomly permuted during the initial 300k training iterations, then linearly anneals to raster between 300k and 600k iterations, and finally sticks to raster order for the subsequent 400k steps. Except for the comparison with Gemma-1, we use the Gemma-2 model series as the backbone transformer for all experiments in this paper.

4.2 Inference

For text decoding, we employ categorical sampling for each generated text prediction. The predicted token is then selected from the vocabulary V based on the sampled probability distribution. We use the same decoding strategy as PaliGemma. Greedy decoding is used for all tasks except for downstream COCOcap (beam search $n=2$) and TextCaps (beam search $n=3$). For image decoding, we use a diffusion sampling process to generate continuous visual tokens. with diffusion sampling step set to 100 in our implementation.

As both text and image generation are performed at the token level, with predictions occurring one token at a time under a causal attention mechanism, we can efficiently utilize Key-Value (KV) caching. This optimization is applicable to both discrete text tokens and continuous visual tokens, significantly accelerating the inference process.

5 Experiment

5.1 Setup

Datasets. We train our models using the WebLI dataset [7], a collection of high-quality image-text pairs. For visual generation, we follow Fluid to employ a WebLI subset of image and text descriptions specifically for the generation task. For visual understanding, consistent with PaliGemma, we leverage the image-text description pairs and image question-answer pairs that are also available within WebLI.

Evaluation Metrics. We assess the image generation quality using the FID [16] score on 30K images of the MS-COCO [24] training set and evaluate performance on the GenEval [13] benchmark, where we use the original text prompt without any rewrites. For evaluating visual understanding performance, we use the caption CIDEr score on MS-COCO. Given our similar training dataset and setup to PaliGemma, we also evaluate the finetuning performance on a variety of captioning and question answering tasks. We report the average score on 4 Captioning tasks, including COCOcap [24], Screen2Words [53], TextCaps [39], WidgetCap [22], and 20 QA tasks, including OKVQA [29], AOKVQA-MC [37], AOKVQA-DA [37], GQA [17], NLVR2 [43], AI2D [19], ScienceQA [28], RSVQA-lr [27], RSVQA-hr (test/test2) [27], ChartQA (human/aug) [30], VizWizVQA [15], Tal-lyQA (simple/complex) [1], CountBenchQA [3], TextVQA [40], DocVQA [32], InfoVQA [31], ST-VQA [4].

In the following sections, we present the experimental results obtained under different configurations of UniFluid, providing insights into the relationship between the two tasks and highlighting key design choices for UniFluid training.

5.2 Main Results

Unified Training Improves Generation Performance. To evaluate the effectiveness of the unified training framework and determine whether unified training offers advantages compared to training separate models for different tasks, we perform controlled experiments to analyze the performance of models trained with a single task.

We first compare the visual generation performance of the model trained under the unified training objective with the performance of a text-to-image model (T2I only), trained solely with the visual

Table 1: Unified training achieves better generation performance than text-to-image only training. We evaluate the performance using MS-COCO zero-shot FID and GenEval score.

| Training Target | Size | FID ↓ | GenEval ↑ |
|-----------------|------|-------------|-------------|
| T2I only | 0.7B | 9.71 | 0.50 |
| Unified | 0.7B | 8.39 | 0.52 |
| T2I only | 2B | 7.88 | 0.59 |
| Unified | 2B | 7.20 | 0.59 |

autoregressive objective for the generation task. We ensure that the total number of visual tokens for training is the same for the visual generation loss in both the unified model training and text-to-image only training scenarios. The generation performance comparison is presented in Table 1. The unified model achieves better performance compared to the T2I only model, despite both models having observed the same number of tokens for the visual generation task. This suggests that unified model training can be beneficial for visual generation tasks, and that visual understanding ability has the potential to unlock enhanced visual generation quality.

Trade-off Between Generation and Understanding. We also investigate whether the visual generation task can contribute to improved visual understanding performance. In the UniFluid unified training setup, the hyperparameter λ controls the balance between the losses applied to image tokens and text tokens.

In Table 3 and Figure 3, we present the understanding and generation results with varying λ of the 0.7B model. We compare the transfer performance to downstream understanding tasks between the unified model with different λ and a image-to-text model (I2T only), trained solely with the image understanding objective. Within the unified training setup, a trade-off exists between visual generation and understanding tasks, which can be effectively controlled by adjusting the loss mixing weight, λ . While increasing λ can improve image understanding performance, ultimately exceeding the I2T-only baseline for downstream captioning, it concurrently diminishes the image generation capabilities.

In most scenarios, a smaller λ value (e.g., 0.005) is advisable, maintaining a significant proportion (over 90%) of image understanding while supporting the generation of high-fidelity images. Larger λ values, in contrast, strongly favor image understanding but result in a rapid drop of image generation ability, as indicated by a sharp rise in FID score when λ exceeds 0.1. Qualitative results for image captioning and question answering, demonstrating the understanding capabilities of the fine-tuned model based on the unified model with Gemma-2 2B as backbone LLM and $\lambda = 0.005$ are presented in Figure 6.

Better Pre-trained LLM Backbone Leads to Better Visual Generation and Understanding. We investigate the effect of pre-trained LLMs within the unified model training setup, specifically examining whether more powerful LLMs contribute to enhanced image understanding performance and superior visual generation quality. To this end, we conducted experiments using Gemma-1 2B [47] and Gemma-2 2B [47] as backbone LLMs. Gemma-2 is a stronger LLM than Gemma-1 with 10% average improvements across different text benchmarks.

Table 2: Performance comparison of image generation and understanding of UniFluid trained with different LLM backbone. FID and CIDEr are measured on MS-COCO. Gemma-2 gets much better performance compared to Gemma-1, for both image understanding and generation tasks.

| Pretrained Model | Generation | | Understanding | | |
|------------------|-------------|-------------|---------------|---------------|--------------|
| | COCO FID ↓ | GenEval ↑ | COCO CIDEr ↑ | Cap Avg ↑ | QA Avg ↑ |
| Gemma-1 | 9.73 | 0.52 | 38.02 | 113.40 | 60.21 |
| Gemma-2 | 7.20 | 0.59 | 40.91 | 116.13 | 62.10 |

The experimental results are presented in Table 2. Here we used $\lambda = 0.005$ for all models. The results demonstrate that employing a stronger LLM is crucial for generating images with higher fidelity and quality. Gemma-2 achieves significantly lower FID scores compared to Gemma-1, highlighting that even though LLM pre-training is unimodal, without exposure to visual data, using a better LLM

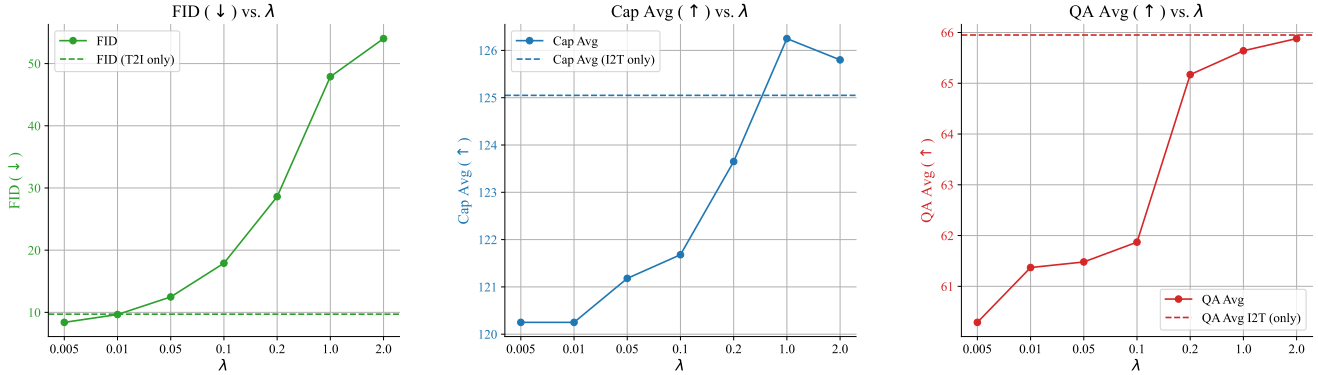


Figure 3: Plot of image understanding and generation performance with varying λ during training. We show the FID on MS-COCO, the average score for downstream captioning tasks (Cap Avg), and the average score for downstream QA tasks (QA Avg) with different λ on the three figures. Green dashed lines shows the FID of T2I-only model, blue and red dashed lines shows the downstream captioning average and QA average for I2T-only model, respectively. In practice, smaller λ has better trade-off between two tasks.

Table 3: Image generation and understanding results with different λ . $\lambda = 0.1$ roughly makes the loss for generation and understanding of the same scale. We present MS-COCO FID and the average captioning and QA results for downstream understanding tasks, compared to the image-to-text (I2T) only baseline. A smaller λ like 0.005 is recommended in most cases as it preserves most of the image understanding capability while enabling the generation of high-quality images and outperforms the text-to-image (T2I) only baseline.

| Task | T2I only | I2T only | Unified, λ | | | | | | |
|------------------------------------|----------|--------------|--------------------|--------|--------|--------|--------|---------------|--------|
| | | | 0.005 | 0.01 | 0.05 | 0.1 | 0.2 | 1.0 | 2.0 |
| Generation (FID) \downarrow | 9.71 | - | 8.39 | 9.65 | 12.48 | 17.90 | 28.60 | 47.89 | 54.02 |
| Understanding (Cap Avg) \uparrow | - | 125.05 | 120.25 | 120.25 | 121.18 | 121.68 | 123.65 | 126.25 | 125.80 |
| Understanding (QA Avg) \uparrow | - | 65.95 | 60.29 | 61.37 | 61.48 | 61.87 | 65.17 | 65.64 | 65.88 |

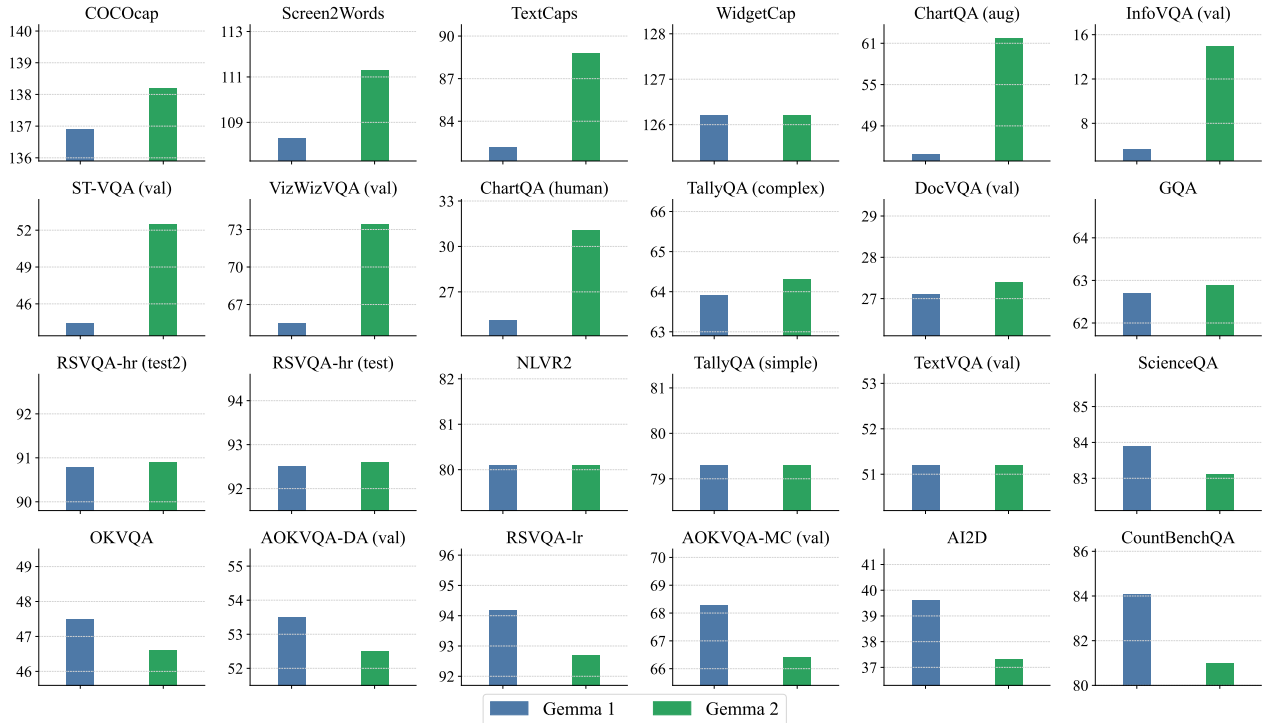


Figure 4: Downstream image understanding performance (after finetuning) on each benchmark (higher is better). Blue bars shows performance of model backbone initialized with Gemma-1 2B and green bars shows model backbone initialized with Gemma-2 2B. Initializing with stronger LLM help improve UniFluid visual understanding performance on most datasets.



A black basketball shoe with a lightning bolt on it.



A melting apple.



A space elevator in the universe.



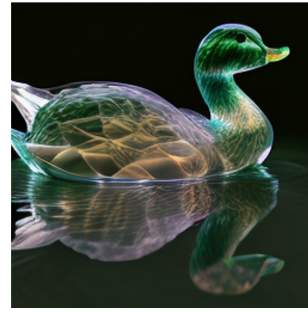
human life depicted entirely out of fractals.



Graffiti of a funny dog on a street wall.



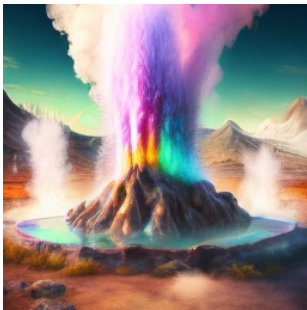
Turtle swimming underwater, aesthetic, fantasy.



A transparent sculpture of a duck made out of glass.



An armchair in the shape of an avocado.



A hyper-detailed rendering of a geyser erupting in a colorful, geothermal landscape.



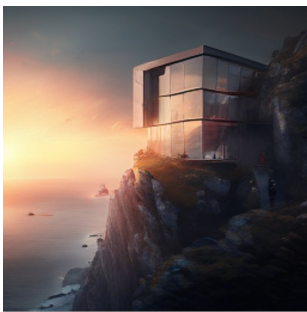
An astronaut riding a horse on the moon, oil painting by Van Gogh.



photo of an eagle with a golden crown resting upon its head.



A window with raindrops trickling down, overlooking a blurry city.



An image of a modern architectural building with large glass windows, situated on a cliff overlooking a serene ocean at sunset.



A cozy cabin in the middle of a snowy forest, surrounded by tall trees with lights glowing through the windows, a northern lights display visible in the sky.



A still life of a vase overflowing with vibrant flowers, painted in bold colors and textured brushstrokes, reminiscent of van Gogh's iconic style.



An otherworldly forest of giant glowing mushrooms under a vibrant night sky filled with distant planets and stars, creating a dreamlike, cosmic landscape.

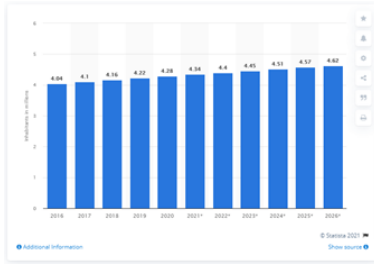
Figure 5: Images generated from UniFluid autoregressive model after aesthetic fine-tuning.



A close up view of a wooden pole with the word "sushi" in silver letters on it. The pole is in front of a parking lot. The pole is in the foreground, with a concrete sidewalk in the foreground. There are plants and trees in the background. There is a brown brick building with a black awning on the left side of it. There are trees in the background. The sky is clear and blue.

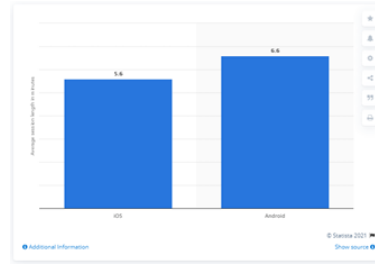


A close up view of a wet white and brown labradoodle dog walking on a gray cement surface. The dog has a red leash attached to its collar. The dog has a silver metal hook attached to its collar. The dog is walking towards the camera. The dog is casting a shadow on the cement surface. Behind the dog is a building with a large window on the side. A tree line is visible in the background. The sky is blue with a few white clouds.



Question: In what year did Panama's population reach 4.28 million?

Answer: 2020



Question: What device's average duration of in-app engagement sessions was 6.6 minutes?

Answer: android



Question: The bus is likely driving through which American city?

Answer: new york



Question: Which number birthday is probably being celebrated?

Answer: thirty

Figure 6: Finetuned UniFluid model demonstrates strong image-to-text capability on image captioning and question answering.



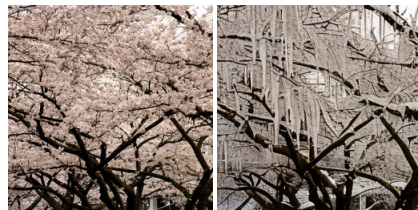
Change the black suitcase to a white one



Remove the fence from the photo



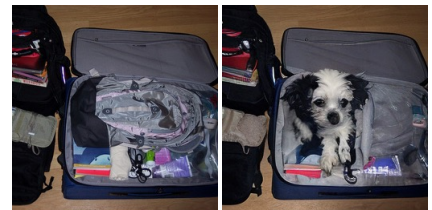
Change this into a 1950s Flintstone cartoon art style



Change the trees from flowers to icicles



Change the elephant into a giant rabbit



Add a puppy on top of the suitcase



Change the bird to all white



Turn it into a Paul Cezanne still life painting



Change the meat into carrots

Figure 7: Image editing results on evaluation benchmark from UniFluid autoregressive model after fine-tuning. It handles multiple editing tasks effectively, including object removal, insertion, style and color changes.

Table 4: Performance comparison of image generation and understanding of UniFluid trained with different image generation order. FID and CIDEr is measured on MS-COCO.

| Generation Order | Generation | | Understanding | | |
|------------------|-------------|-----------|---------------|---------------|--------------|
| | COCO FID ↓ | GenEval ↑ | COCO CIDEr ↑ | Cap Avg ↑ | QA Avg ↑ |
| Raster | 8.28 | 0.59 | 45.57 | 116.55 | 61.81 |
| Random | 7.20 | 0.59 | 40.91 | 116.13 | 62.10 |

as a backbone is important for unlocking improved visual quality in a unified model training setup. The image understanding performance also improved slightly when using stronger LLM, which is a trend also noted in PaliGemma2. We show the detailed comparison on each downstream visual understanding benchmark in Figure 4.

Training with Random Order Helps Generation But Not Understanding. Images inherently possess 2D patterns. As demonstrated in Fluid, raster-order training can be problematic, potentially leading to collapse and artifacts characterized by disappearing patterns. Approaches such as RAR [58] and RandAR [33] propose training image generation AR models with random-order training, which can improve ImageNet FID and result in better visual quality.

Here we study the effect of different visual generation orders during training within our unified framework setup. We compare the performance between random-order and raster-order training, both with Gemma-2 2B as backbone LLM. The results presented in Table 4 indicate that for per-token image generation within a unified framework, raster-order training continues to underperform compared to random-order generation. Incorporating random-order during training could ensure the generated images are of high quality. However, it does not necessarily improve the visual understanding performance, where raster-order achieves better performance on MS-COCO CIDEr and downstream captioning task average (Cap Avg).

5.3 More Generation Capabilities

We also verify the transferability of the trained model to various downstream generation tasks.

Aesthetic Fine-Tuning. To enhance the visual quality and aesthetic appeal of the generated images, we perform aesthetic fine-tuning on a publicly available dataset. The results are shown in Figure 5.

Image Editing Task. Since our unified framework is trained with multimodal inputs, it can naturally extend to image editing tasks that involve both image and text prompt inputs. We fine-tune the 2B UniFluid model with 4M image editing pairs from HQEdit [18] and UltraEdit [60]. In Figure 7, we apply the fine-tuned model to the input images and editing prompts from a public available benchmark. Although preliminary, the experiments show that UniFluid is able to adapt and generalize to tasks that involve interleaved data modalities.

6 Conclusion

In this paper, we presented UniFluid, a pure autoregressive framework for joint visual generation and understanding, utilizing continuous visual tokens. We identified an inherent trade-off between the visual generation and understanding tasks, but the two tasks can benefit each other with tuned training recipes. Careful choice of the loss balance between the two tasks allows a single unified model to achieve performance comparable to or exceeding single-task baselines. We conducted investigation of key design choices for UniFluid training, revealing the critical importance of employing strong backbone LLM and random-order generation to unlock high-quality visual generation capabilities. We believe that this work encourages future research into the exploration of continuous visual tokens for unified vision-language model training, paving the way for more efficient and powerful autoregressive multimodal systems.

Acknowledgements. We are grateful to Alex Rizkowsky and Amy Shen for their support in securing computational resources. We also wish to thank Charles Herrmann, Junhwa Hur, Shangbang Long, André Susano Pinto, Srinivas Kaza, David Salesin, and the VisCam team for their insightful discussions and constructive feedback, which greatly improved this work.

References

- [1] Manoj Acharya, Kushal Kafle, and Christopher Kanan. Tallyqa: Answering complex counting questions. In *Proceedings of the AAAI conference on artificial intelligence*, volume 33, pages 8076–8084, 2019.
- [2] Jean-Baptiste Alayrac, Jeff Donahue, Pauline Luc, Antoine Miech, Iain Barr, Yana Hasson, Karel Lenc, Arthur Mensch, Katherine Millican, Malcolm Reynolds, et al. Flamingo: a visual language model for few-shot learning. *Advances in neural information processing systems*, 35:23716–23736, 2022.
- [3] Lucas Beyer, Andreas Steiner, André Susano Pinto, Alexander Kolesnikov, Xiao Wang, Daniel Salz, Maxim Neumann, Ibrahim Alabdulmohsin, Michael Tschannen, Emanuele Bugliarello, et al. Paligemma: A versatile 3b vlm for transfer. *arXiv preprint arXiv:2407.07726*, 2024.
- [4] Ali Furkan Biten, Ruben Tito, Andres Mafla, Lluís Gomez, Marçal Rusinol, Ernest Valveny, CV Jawahar, and Dimosthenis Karatzas. Scene text visual question answering. In *Proceedings of the IEEE/CVF international conference on computer vision*, pages 4291–4301, 2019.
- [5] Tom Brown, Benjamin Mann, Nick Ryder, Melanie Subbiah, Jared D Kaplan, Prafulla Dhariwal, Arvind Neelakantan, Pranav Shyam, Girish Sastry, Amanda Askell, et al. Language models are few-shot learners. *Advances in neural information processing systems*, 33:1877–1901, 2020.
- [6] Huiwen Chang, Han Zhang, Jarred Barber, AJ Maschinot, Jose Lezama, Lu Jiang, Ming-Hsuan Yang, Kevin Murphy, William T Freeman, Michael Rubinstein, et al. Muse: Text-to-image generation via masked generative transformers. *arXiv preprint arXiv:2301.00704*, 2023.
- [7] Xi Chen, Xiao Wang, Soravit Changpinyo, AJ Piergiovanni, Piotr Padlewski, Daniel Salz, Sebastian Goodman, Adam Grycner, Basil Mustafa, Lucas Beyer, et al. Pali: A jointly-scaled multilingual language-image model. *arXiv preprint arXiv:2209.06794*, 2022.
- [8] Xiaokang Chen, Zhiyu Wu, Xingchao Liu, Zizheng Pan, Wen Liu, Zhenda Xie, Xingkai Yu, and Chong Ruan. Janus-pro: Unified multimodal understanding and generation with data and model scaling. *arXiv preprint arXiv:2501.17811*, 2025.
- [9] Aakanksha Chowdhery, Sharan Narang, Jacob Devlin, Maarten Bosma, Gaurav Mishra, Adam Roberts, Paul Barham, Hyung Won Chung, Charles Sutton, Sebastian Gehrmann, et al. Palm: Scaling language modeling with pathways. *Journal of Machine Learning Research*, 24(240):1–113, 2023.
- [10] Wenliang Dai, Junnan Li, Dongxu Li, Anthony Meng Huat Tiong, Junqi Zhao, Weisheng Wang, Boyang Li, Pascale Fung, and Steven Hoi. Instructblip: Towards general-purpose vision-language models with instruction tuning, 2023.
- [11] Jacob Devlin, Ming-Wei Chang, Kenton Lee, and Kristina Toutanova. Bert: Pre-training of deep bidirectional transformers for language understanding. In *Proceedings of the 2019 conference of the North American chapter of the association for computational linguistics: human language technologies, volume 1 (long and short papers)*, pages 4171–4186, 2019.
- [12] Lijie Fan, Tianhong Li, Siyang Qin, Yuanzhen Li, Chen Sun, Michael Rubinstein, Deqing Sun, Kaiming He, and Yonglong Tian. Fluid: Scaling autoregressive text-to-image generative models with continuous tokens. *arXiv preprint arXiv:2410.13863*, 2024.
- [13] Dhruva Ghosh, Hannaneh Hajishirzi, and Ludwig Schmidt. Geneval: An object-focused framework for evaluating text-to-image alignment. *Advances in Neural Information Processing Systems*, 36:52132–52152, 2023.
- [14] Karol Gregor, Ivo Danihelka, Andriy Mnih, Charles Blundell, and Daan Wierstra. Deep autoregressive networks. In *International Conference on Machine Learning*, pages 1242–1250. PMLR, 2014.
- [15] Danna Gurari, Qing Li, Abigale J Stangl, Anhong Guo, Chi Lin, Kristen Grauman, Jiebo Luo, and Jeffrey P Bigham. Vizwiz grand challenge: Answering visual questions from blind people. In *Proceedings of the IEEE conference on computer vision and pattern recognition*, pages 3608–3617, 2018.

- [16] Martin Heusel, Hubert Ramsauer, Thomas Unterthiner, Bernhard Nessler, and Sepp Hochreiter. Gans trained by a two time-scale update rule converge to a local nash equilibrium. *Advances in neural information processing systems*, 30, 2017.
- [17] Drew A Hudson and Christopher D Manning. Gqa: A new dataset for real-world visual reasoning and compositional question answering. In *Proceedings of the IEEE/CVF conference on computer vision and pattern recognition*, pages 6700–6709, 2019.
- [18] Mude Hui, Siwei Yang, Bingchen Zhao, Yichun Shi, Heng Wang, Peng Wang, Yuyin Zhou, and Cihang Xie. Hq-edit: A high-quality dataset for instruction-based image editing. *arXiv preprint arXiv:2404.09990*, 2024.
- [19] Aniruddha Kembhavi, Mike Salvato, Eric Kolve, Minjoon Seo, Hannaneh Hajishirzi, and Ali Farhadi. A diagram is worth a dozen images. In *Computer Vision—ECCV 2016: 14th European Conference, Amsterdam, The Netherlands, October 11–14, 2016, Proceedings, Part IV 14*, pages 235–251. Springer, 2016.
- [20] Taku Kudo and John Richardson. Sentencepiece: A simple and language independent subword tokenizer and detokenizer for neural text processing. *arXiv preprint arXiv:1808.06226*, 2018.
- [21] Tianhong Li, Yonglong Tian, He Li, Mingyang Deng, and Kaiming He. Autoregressive image generation without vector quantization. *Advances in Neural Information Processing Systems*, 37:56424–56445, 2024.
- [22] Yang Li, Gang Li, Luheng He, Jingjie Zheng, Hong Li, and Zhiwei Guan. Widget captioning: Generating natural language description for mobile user interface elements. *arXiv preprint arXiv:2010.04295*, 2020.
- [23] Ji Lin, Hongxu Yin, Wei Ping, Pavlo Molchanov, Mohammad Shoeybi, and Song Han. Vila: On pre-training for visual language models. In *Proceedings of the IEEE/CVF conference on computer vision and pattern recognition*, pages 26689–26699, 2024.
- [24] Tsung-Yi Lin, Michael Maire, Serge Belongie, James Hays, Pietro Perona, Deva Ramanan, Piotr Dollár, and C Lawrence Zitnick. Microsoft coco: Common objects in context. In *Computer vision—ECCV 2014: 13th European conference, zurich, Switzerland, September 6-12, 2014, proceedings, part v 13*, pages 740–755. Springer, 2014.
- [25] Haotian Liu, Chunyuan Li, Yuheng Li, and Yong Jae Lee. Improved baselines with visual instruction tuning. In *Proceedings of the IEEE/CVF Conference on Computer Vision and Pattern Recognition*, pages 26296–26306, 2024.
- [26] Haotian Liu, Chunyuan Li, Qingyang Wu, and Yong Jae Lee. Visual instruction tuning. *Advances in neural information processing systems*, 36:34892–34916, 2023.
- [27] Sylvain Lobry, Diego Marcos, Jesse Murray, and Devis Tuia. Rsvqa: Visual question answering for remote sensing data. *IEEE Transactions on Geoscience and Remote Sensing*, 58(12):8555–8566, 2020.
- [28] Pan Lu, Swaroop Mishra, Tanglin Xia, Liang Qiu, Kai-Wei Chang, Song-Chun Zhu, Oyvind Tafjord, Peter Clark, and Ashwin Kalyan. Learn to explain: Multimodal reasoning via thought chains for science question answering. *Advances in Neural Information Processing Systems*, 35:2507–2521, 2022.
- [29] Kenneth Marino, Mohammad Rastegari, Ali Farhadi, and Roozbeh Mottaghi. Ok-vqa: A visual question answering benchmark requiring external knowledge. In *Proceedings of the IEEE/cvf conference on computer vision and pattern recognition*, pages 3195–3204, 2019.
- [30] Ahmed Masry, Do Xuan Long, Jia Qing Tan, Shafiq Joty, and Enamul Hoque. Chartqa: A benchmark for question answering about charts with visual and logical reasoning. *arXiv preprint arXiv:2203.10244*, 2022.
- [31] Minesh Mathew, Viraj Bagal, Rubèn Tito, Dimosthenis Karatzas, Ernest Valveny, and CV Jawahar. Infographicvqa. In *Proceedings of the IEEE/CVF Winter Conference on Applications of Computer Vision*, pages 1697–1706, 2022.

- [32] Minesh Mathew, Dimosthenis Karatzas, and CV Jawahar. Docvqa: A dataset for vqa on document images. In *Proceedings of the IEEE/CVF winter conference on applications of computer vision*, pages 2200–2209, 2021.
- [33] Ziqi Pang, Tianyuan Zhang, Fujun Luan, Yunze Man, Hao Tan, Kai Zhang, William T Freeman, and Yu-Xiong Wang. Randar: Decoder-only autoregressive visual generation in random orders. *arXiv preprint arXiv:2412.01827*, 2024.
- [34] Niki Parmar, Ashish Vaswani, Jakob Uszkoreit, Lukasz Kaiser, Noam Shazeer, Alexander Ku, and Dustin Tran. Image transformer. In *International conference on machine learning*, pages 4055–4064. PMLR, 2018.
- [35] Alec Radford, Karthik Narasimhan, Tim Salimans, and Ilya Sutskever. Improving language understanding by generative pre-training. *Technical Report*, 2018.
- [36] Robin Rombach, Andreas Blattmann, Dominik Lorenz, Patrick Esser, and Björn Ommer. High-resolution image synthesis with latent diffusion models, 2021.
- [37] Dustin Schwenk, Apoorv Khandelwal, Christopher Clark, Kenneth Marino, and Roozbeh Mottaghi. A-okvqa: A benchmark for visual question answering using world knowledge. In *European conference on computer vision*, pages 146–162. Springer, 2022.
- [38] Weijia Shi, Xiaochuang Han, Chunting Zhou, Weixin Liang, Xi Victoria Lin, Luke Zettlemoyer, and Lili Yu. Llamafusion: Adapting pretrained language models for multimodal generation. *arXiv preprint arXiv:2412.15188*, 2024.
- [39] Oleksii Sidorov, Ronghang Hu, Marcus Rohrbach, and Amanpreet Singh. Textcaps: a dataset for image captioning with reading comprehension. In *Computer Vision—ECCV 2020: 16th European Conference, Glasgow, UK, August 23–28, 2020, Proceedings, Part II 16*, pages 742–758. Springer, 2020.
- [40] Amanpreet Singh, Vivek Natarajan, Meet Shah, Yu Jiang, Xinlei Chen, Dhruv Batra, Devi Parikh, and Marcus Rohrbach. Towards vqa models that can read. In *Proceedings of the IEEE/CVF conference on computer vision and pattern recognition*, pages 8317–8326, 2019.
- [41] Yang Song, Jascha Sohl-Dickstein, Diederik P Kingma, Abhishek Kumar, Stefano Ermon, and Ben Poole. Score-based generative modeling through stochastic differential equations. *arXiv preprint arXiv:2011.13456*, 2020.
- [42] Andreas Steiner, André Susano Pinto, Michael Tschannen, Daniel Keysers, Xiao Wang, Yonatan Bitton, Alexey Gritsenko, Matthias Minderer, Anthony Sherbondy, Shangbang Long, et al. Paligemma 2: A family of versatile vlms for transfer. *arXiv preprint arXiv:2412.03555*, 2024.
- [43] Alane Suhr, Stephanie Zhou, Ally Zhang, Iris Zhang, Huajun Bai, and Yoav Artzi. A corpus for reasoning about natural language grounded in photographs. *arXiv preprint arXiv:1811.00491*, 2018.
- [44] Quan Sun, Qiyang Yu, Yufeng Cui, Fan Zhang, Xiaosong Zhang, Yueze Wang, Hongcheng Gao, Jingjing Liu, Tiejun Huang, and Xinlong Wang. Emu: Generative pretraining in multimodality. *arXiv preprint arXiv:2307.05222*, 2023.
- [45] Yutao Sun, Hangbo Bao, Wenhui Wang, Zhiliang Peng, Li Dong, Shaohan Huang, Jianyong Wang, and Furu Wei. Multimodal latent language modeling with next-token diffusion. *arXiv preprint arXiv:2412.08635*, 2024.
- [46] Chameleon Team. Chameleon: Mixed-modal early-fusion foundation models. *arXiv preprint arXiv:2405.09818*, 2024.
- [47] Gemma Team, Thomas Mesnard, Cassidy Hardin, Robert Dadashi, Surya Bhupatiraju, Shreya Pathak, Laurent Sifre, Morgane Rivière, Mihir Sanjay Kale, Juliette Love, et al. Gemma: Open models based on gemini research and technology. *arXiv preprint arXiv:2403.08295*, 2024.

- [48] Gemma Team, Morgane Riviere, Shreya Pathak, Pier Giuseppe Sessa, Cassidy Hardin, Surya Bhupatiraju, Léonard Hussenot, Thomas Mesnard, Bobak Shahriari, Alexandre Ramé, et al. Gemma 2: Improving open language models at a practical size. *arXiv preprint arXiv:2408.00118*, 2024.
- [49] Keyu Tian, Yi Jiang, Zehuan Yuan, Bingyue Peng, and Liwei Wang. Visual autoregressive modeling: Scalable image generation via next-scale prediction. *Advances in neural information processing systems*, 37:84839–84865, 2024.
- [50] Shengbang Tong, David Fan, Jiachen Zhu, Yunyang Xiong, Xinlei Chen, Koustuv Sinha, Michael Rabbat, Yann LeCun, Saining Xie, and Zhuang Liu. Metamorph: Multimodal understanding and generation via instruction tuning. *arXiv preprint arXiv:2412.14164*, 2024.
- [51] Aaron Van den Oord, Nal Kalchbrenner, Lasse Espeholt, Oriol Vinyals, Alex Graves, et al. Conditional image generation with pixelcnn decoders. *Advances in neural information processing systems*, 29, 2016.
- [52] Aäron Van Den Oord, Nal Kalchbrenner, and Koray Kavukcuoglu. Pixel recurrent neural networks. In *International conference on machine learning*, pages 1747–1756. PMLR, 2016.
- [53] Bryan Wang, Gang Li, Xin Zhou, Zhouong Chen, Tovi Grossman, and Yang Li. Screen2words: Automatic mobile ui summarization with multimodal learning. In *The 34th Annual ACM Symposium on User Interface Software and Technology*, pages 498–510, 2021.
- [54] Chengyue Wu, Xiaokang Chen, Zhiyu Wu, Yiyang Ma, Xingchao Liu, Zizheng Pan, Wen Liu, Zhenda Xie, Xingkai Yu, Chong Ruan, et al. Janus: Decoupling visual encoding for unified multimodal understanding and generation. *arXiv preprint arXiv:2410.13848*, 2024.
- [55] Jinheng Xie, Weijia Mao, Zechen Bai, David Junhao Zhang, Weihao Wang, Kevin Qinghong Lin, Yuchao Gu, Zhijie Chen, Zhenheng Yang, and Mike Zheng Shou. Show-o: One single transformer to unify multimodal understanding and generation. *arXiv preprint arXiv:2408.12528*, 2024.
- [56] Qinghao Ye, Haiyang Xu, Guohai Xu, Jiabo Ye, Ming Yan, Yiyang Zhou, Junyang Wang, Anwen Hu, Pengcheng Shi, Yaya Shi, et al. mplug-owl: Modularization empowers large language models with multimodality. *arXiv preprint arXiv:2304.14178*, 2023.
- [57] Jiahui Yu, Yuanzhong Xu, Jing Yu Koh, Thang Luong, Gunjan Baid, Zirui Wang, Vijay Vasudevan, Alexander Ku, Yinfei Yang, Burcu Karagol Ayan, et al. Scaling autoregressive models for content-rich text-to-image generation. *arXiv preprint arXiv:2206.10789*, 2(3):5, 2022.
- [58] Qihang Yu, Ju He, Xueqing Deng, Xiaohui Shen, and Liang-Chieh Chen. Randomized autoregressive visual generation. *arXiv preprint arXiv:2411.00776*, 2024.
- [59] Xiaohua Zhai, Basil Mustafa, Alexander Kolesnikov, and Lucas Beyer. Sigmoid loss for language image pre-training. In *Proceedings of the IEEE/CVF international conference on computer vision*, pages 11975–11986, 2023.
- [60] Haozhe Zhao, Xiaojian Shawn Ma, Liang Chen, Shuzheng Si, Rujie Wu, Kaikai An, Peiyu Yu, Minjia Zhang, Qing Li, and Baobao Chang. Ultraedit: Instruction-based fine-grained image editing at scale. *Advances in Neural Information Processing Systems*, 37:3058–3093, 2024.
- [61] Chunting Zhou, Lili Yu, Arun Babu, Kushal Tirumala, Michihiro Yasunaga, Leonid Shamis, Jacob Kahn, Xuezhe Ma, Luke Zettlemoyer, and Omer Levy. Transfusion: Predict the next token and diffuse images with one multi-modal model. *arXiv preprint arXiv:2408.11039*, 2024.
- [62] Deyao Zhu, Jun Chen, Xiaoqian Shen, Xiang Li, and Mohamed Elhoseiny. Minigpt-4: Enhancing vision-language understanding with advanced large language models. *arXiv preprint arXiv:2304.10592*, 2023.